



Master Thesis

Jian Wu – xcb479@alumni.ku.dk

Deep Contact

Accelerating Rigid Simulation with Convolutional Networks

Supervisor: Kenny Erleben

August 6th 2018



Abstract

This is a master theis from

Contents

1	Introdustion	1
1.1	Motivation	1
1.2	Thesis Overview	1
2	Rigid Body Dynamics Simulation	2
2.1	Rigid dynamics Simulation	2
2.1.1	Simulation Basics	2
2.1.2	Rigid Body Concepts	3
2.1.3	Rigid Body Equations of Motions	3
2.1.4	Twist/Wrench	5
2.1.5	Newton-Euler Equation	5
2.2	Constrained Dynamics	6
2.2.1	Expressing Constraints as Equations	6
2.2.2	contact Constraints	6
2.2.3	7
3	Particle-grid-particle	8
3.1	Grid-Based method	8
3.2	Smoothed Particle Hydrodynamics	8
3.2.1	Fundamentals	9
3.2.2	Kernels	10
3.2.3	Grid size and smoothing length	11
3.2.4	Neighbor Search	11
3.3	Grid to particle	13
3.3.1	Bilinear interpolation	14
3.4	Conclusion	15
4	Deep Learning For Simulation	16
4.1	Convolutional Neural Networks	16
4.2	CNN Constructure	16
4.2.1	Convolutional layers	16

4.2.2	Full-connected layers	16
4.3	Trainig configuration	16
4.3.1	Loss Function	16
4.3.2	Optimizer(SGD)	16
4.4	Training Results	16
4.5	Simulation based on Trained model	16
5	Implementation	17
6	Conclusion	18
6.1	Future work	18
	References	19

List of Figures

3.1	Grid description, <i>retrieved from MIT</i> (2011)	8
3.2	Visilaztion of SPH	9
3.3	Comparation of different kernels, we set smoothing length $h = 1$ here.	12
3.4	Comparation of gradient of different kernels, we set $h = 1$ here.	13
3.5	The figure shows visiualization of bilinear interpola- tion. The four red dots show the data points and the green dot is the point at which we want to interpolate.	14

List of Tables

Chapter 1

Introduction

1.1 Motivation

Movies studios have been pushing facial and character animation to a level where machine learning can automate a large part of this work in a production pipeline. Research community is exploring machine learning for gait control too and quite successfully or for upscaling of liquid simulation[1].

However, for rigid body problems it is not quite clear how to approach the technicalities in applying deep learning. Some work have been done in terms of inverse simulations or pilings to control rigid bodies to perform a given artistic ‘target’. These techniques are more in spirit of inverse problems that maps initial conditions to a well defined outcome(number of bounces or which face up on a cube) or level of detail idea replacing interiors of piles with stacks of cylinders of decreasing radius to make an overall apparent pile have a given angle of repose.

1.2 Thesis Overview

This thesis explore the application of convolutional neural networks in Computer Simulation.

Chapter 2

Rigid Body Dynamics Simulation

This chapter mainly introduces rigid body simulation to help you understand how computer simulate rigid dynamics based on traditional newton-euler equations. For more details, some contact forces solvers are described in this chapter. Afterwards, we will use one of solver to run some simulation and get the image data for the next step, grids-transfer. All the discussion about rigid simulation and contacts solver are based on 2- D view.

2.1 Rigid dynamics Simulation

2.1.1 Simulation Basics

Simulating the motion of a rigid body is almost the same as simulating the motion of a particle, so I will start with particle simulation. For particle simulation, we let function $\mathbf{x}(t)$ describe the particle's location in world space at time t . Then we use $\mathbf{v}(t) = \frac{d}{dt}\mathbf{x}(t)$ to denote the velocity of the particle at time t . So, the state of a particle at a time t is the particle's position and velocity. We generalize this concept by defining a state vector $\mathbf{Y}(t)$ for a system: for a single particle,

$$\mathbf{Y}(t) = \begin{pmatrix} \mathbf{x}_1(t) \\ \mathbf{v}_1(t) \end{pmatrix} \quad (2.1)$$

For a system with n particles, we enlarge $\mathbf{Y}(t)$ to be

$$\mathbf{Y}(t) = \begin{pmatrix} \mathbf{x}_1(t) \\ \mathbf{v}_1(t) \\ \dots \\ \mathbf{x}_n(t) \\ \mathbf{v}_n(t) \end{pmatrix} \quad (2.2)$$

However, to simulate the motion of particles actually, we need to know one more thing – the forces. $\mathbf{F}(t)$ is defined as the force acting on the particle. If the mass of the particle is m , then the changes of $\mathbf{Y}(t)$ will be given by

$$\frac{d}{dt}\mathbf{Y}(t) = \frac{d}{dt} \begin{pmatrix} \mathbf{x}(t) \\ \mathbf{v}(t) \end{pmatrix} = \begin{pmatrix} \mathbf{v}(t) \\ \mathbf{F}(t)/m \end{pmatrix} \quad (2.3)$$

2.1.2 Rigid Body Concepts

Unlike a particle, a rigid body occupies a volume of space and has a particular shape. Rigid bodies are more complicated, beside translating them, we can rotate them as well. To locate a rigid body, we use $\mathbf{x}(t)$ to denote their translation and a rotation matrix $\mathbf{R}(t)$ to describe their rotation.

2.1.3 Rigid Body Equations of Motions

Whereas linear momentum $\mathbf{P}(t)$ is related to linear velocity with a scalar (the mass), angular momentum is related to angular velocity with a matrix \mathbf{I} , called the angular inertia matrix. The reason for this is that objects generally have different angular inertias around different axes of rotation. Angular momentum is defined as \mathbf{L} . The linear momentum is defined as 2.4, and angular momentum is defined as 2.5

$$\mathbf{P}(t) = m\mathbf{v}(t) \quad (2.4)$$

$$\mathbf{L}(t) = \mathbf{I}(t)\boldsymbol{\omega}(t) \quad (2.5)$$

The total torque $\boldsymbol{\tau}$ applied to the body is equal to the rate of change of the angular momentum, as defined in 2.6:

$$\boldsymbol{\tau} = \frac{d}{dt}\mathbf{L} = \frac{d}{dt}(\mathbf{I}\boldsymbol{\omega}) \quad (2.6)$$

Then we can covert all concepts we need to define stare \mathbf{Y} for a rigid body.

$$\mathbf{Y}(t) = \begin{pmatrix} \mathbf{x}(t) \\ \mathbf{R}(t) \\ \mathbf{P}(t) \\ \mathbf{L}(t) \end{pmatrix} \quad (2.7)$$

Like what is epressed in $\mathbf{Y}(t)$, the state of a rigid body is mainly consist by its position and orientation (describing spatial information), and its linear and angualr momentum(describe velocity information). Since mass m and bodyspace inertia tensor \mathbf{I}_{body} are constants, we can the auxiliary quantities $\mathbf{I}(t)$, $\boldsymbol{\omega}(t)$ at any given time.

$$\mathbf{v}(t) = \frac{\mathbf{P}(t)}{m} \quad \mathbf{I}(t) = \mathbf{R}(t)\mathbf{I}_{body}\mathbf{R}(t)^T \quad \boldsymbol{\omega}(t) = \mathbf{I}(t)^{-1}\mathbf{L}(t) \quad (2.8)$$

The derivative $\frac{d}{dt}\mathbf{Y}(t)$ is

$$\frac{d}{dt}\mathbf{Y}(t) = \frac{d}{dt} \begin{pmatrix} \mathbf{x}(t) \\ \mathbf{R}(t) \\ m\mathbf{v}(t) \\ \mathbf{L}(t) \end{pmatrix} = \frac{d}{dt} \begin{pmatrix} \mathbf{v}(t) \\ \boldsymbol{\omega}(t) \times \mathbf{R}(t) \\ \mathbf{F}(t) \\ \boldsymbol{\tau}(t) \end{pmatrix} \quad (2.9)$$

Then, we can evaluate Equation 2.10 as follows:

$$\begin{aligned} \boldsymbol{\tau} &= \frac{d}{dt}(\mathbf{I}\boldsymbol{\omega}) \\ &= \mathbf{I}\dot{\boldsymbol{\omega}} + \dot{\mathbf{I}}\boldsymbol{\omega} \\ &= \mathbf{I}\dot{\boldsymbol{\omega}} + \frac{d}{dt}(\mathbf{R}\mathbf{I}_{body}\mathbf{R}^T)\boldsymbol{\omega} \\ &= \mathbf{I}\dot{\boldsymbol{\omega}} + (\dot{\mathbf{R}}\mathbf{I}_{body}\mathbf{R}^T + \mathbf{R}\mathbf{I}_{body}\dot{\mathbf{R}}^T)\boldsymbol{\omega} \\ &= \mathbf{I}\dot{\boldsymbol{\omega}} + ([\boldsymbol{\omega}]\mathbf{R}\mathbf{I}_{body}\mathbf{R}^T + \mathbf{R}\mathbf{I}_{body}\mathbf{R}^T\hat{\boldsymbol{\omega}})\boldsymbol{\omega} \\ &= \mathbf{I}\dot{\boldsymbol{\omega}} + [\boldsymbol{\omega}]\mathbf{I}\boldsymbol{\omega} - \mathbf{I}[\boldsymbol{\omega}]\boldsymbol{\omega} \end{aligned} \quad (2.10)$$

Since $\boldsymbol{\omega} \times \boldsymbol{\omega}$ is zero, the final term can be cancels out. This relationship left is knowned as :

$$\boldsymbol{\tau} = \mathbf{I}\dot{\boldsymbol{\omega}} + [\boldsymbol{\omega}]\mathbf{I}\boldsymbol{\omega} \quad (2.11)$$

2.1.4 Twist/Wrench

We will now introduce vectors called twists, which describe velocities, and wrenches, which describe forces, and explain how these objects transform from one coordinate frame to another one.

Twist

A twist is a vector that expresses rigid motion or velocity. In Section 2.2, we saw how to parameterize the velocity of a rigid body as a linear velocity vector and an angular velocity vector. The coordinates of a twist are given as a 4-vector in 2-D simulation, which we can check in 2.12

$$\mathbf{v} = \begin{pmatrix} \boldsymbol{\omega} \\ \mathbf{v} \end{pmatrix} \quad (2.12)$$

. The definition can be found in 2.12, containing a linear velocity vector \mathbf{v} and an angular velocity $\boldsymbol{\omega}$. According to

Wrench

A wrench is a vector that expresses force and torque acting on a body. A wrench can be defined by

$$\mathbf{f} = \begin{pmatrix} \boldsymbol{\tau} \\ \mathbf{f} \end{pmatrix} \quad (2.13)$$

A wrench contains an angular component $\boldsymbol{\tau}$ and a linear component \mathbf{f} , which are applied at the origin of the coordinate frame they are specified in.

2.1.5 Newton-Euler Equation

The Newton-Euler equations for a rigid body can now be written in terms of the body's acceleration twist $\dot{\mathbf{v}}$ mentioned in 2.12 and the wrench \mathbf{f} mentioned in ?? acting on the body. We can simply write the Newton and Euler equations,

$$\begin{pmatrix} \boldsymbol{\tau} - \boldsymbol{\omega} \times \mathbf{I}\boldsymbol{\omega} \\ \mathbf{f} \end{pmatrix} = \begin{pmatrix} \mathbf{I} & \mathbf{0} \\ \mathbf{0} & m\mathbf{1}_{2 \times 2} \end{pmatrix} \dot{\mathbf{v}} \quad (2.14)$$

if we define \mathbf{M} and \mathbf{g} as Equation ?? and ??

$$\mathbf{M} \triangleq [\quad (2.15)$$

2.2 Constrained Dynamics

most interesting simulations of rigid bodies involve some kind of constraints. Usually we want to model systems of bodies that are interacting in some way. Some bodies may be in contact with each other, or attached together by some types of joint. Since this report mainly research contact forces, we

2.2.1 Expressing Constraints as Equations

We express constraints mathematically as algebraic matrix equations with position, velocity, or acceleration vectors as the unknowns. In general, the configuration space of a set of n rigid bodies has dimension $6n$. Adding constraint equations restricts the position (or velocity, or acceleration) to a subspace of smaller dimension.

The constraints discussed in this thesis will all be holonomic constraints, which means the constraint on the velocity can be found by taking the derivative of a position constraint. Constraints that do not fit this description are called nonholonomic. An example of a nonholonomic constraint is a ball rolling on a table without slipping. The position of the ball has five degrees of freedom, so there is only one degree of constraint (only the height is constrained). Taking the derivative of the position constraint would only give a velocity constraint of degree one. Additional constraints on the velocity are needed to prevent the ball from slipping.

We will describe position constraints with a constraint function $g(\mathbf{p})$, which is a function from the space of possible positions of the rigid bodies, to \mathbf{R}^d , where d is the number of degrees of freedom that constraint removes from the dynamic system. If the constraint function returns a zero vector, then

2.2.2 contact Constraints

- A contact consist of a pair of contact points, one point attached, one point attached to one rigid body, and the other point attached to another rigid body. The contact points are sufficiently close together for our collision detection algorithm to report a collision.
- A contact normal is a unit vector that is normal to one or both of the surfaces at the contact points.

- The contact constraint Jacobian for constraint i , denoted by \mathbf{J}_{c_i} , is a $1 \times 6n$ matrix, where n is the number of bodies (the subscript ‘ c ’ here stands for ‘contact’).
- A contact force $\mathbf{J}_{c_i}^T \lambda_{c_i}$ is a force acting in the direction of the contact normal which prevents the two rigid bodies from interpenetrating.
- The separation distance of a contact is the normal component of the distance between the two contact points. It is negative when the bodies are interpenetrating at the contact. The constraint function $g_i()$ for a contact constraint returns the separation distance. In other words, $g_i \geq 0$.
- The relative normal acceleration a_i of a contact is the second derivative of the separation distance with respect to time ($a_i = \ddot{g}_i$). The acceleration constraint is satisfied when $a_i = \mathbf{J}_{c_i} \dot{\mathbf{v}} + k_i \geq 0$

2.2.3

Chapter 3

Particle-grid-particle

The basic method for generating training data which is more accessible to learning is that we will map a discrete element method (DEM) into a continuum setting use techniques from smooth particle hydrodynamics. Given a set of bodies δ and a set of contacts between these bodies C .

3.1 Grid-Based method

Traditional rigid motion simulation mainly use particle-based method. However, if we want to replace traditional contact solver with deep learning model, it is hard for cnn model to recognize the original image and do learning. Grid-based method is a good to transfer original image to a grid-cells and then use

3.2 Smoothed Particle Hydrodynamics

Smoothed particle hydrodynamics (SPH) was invented to simulate nonaxisymmetric phenomena in astrophysics initially. The principal

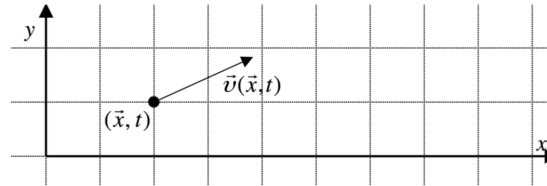


Figure 3.1: Grid description, *retrieved from MIT* (2011)

idea of SPH is to treat hydrodynamics in a completely mesh-free fashion, in terms of a set of sampling particles. It turns out that the particle presentation of SPH has excellent conservation properties. Energy, linear momentum, angular momentum, mass and velocity.

3.2.1 Fundamentals

At the heart of SPH is a kernel interpolation method which allows any function to be expressed in terms of its values at a set of disordered points - the particles[2]. For a field $A(\mathbf{r})$, a smoothed interpolated version $A_I(\mathbf{r})$ can be defined by a kernel $W(\mathbf{r}, h)$,

$$A_I(\mathbf{r}) = \int A(\mathbf{r}') W(\|\mathbf{r} - \mathbf{r}'\|, h) d\mathbf{r}' \quad (3.1)$$

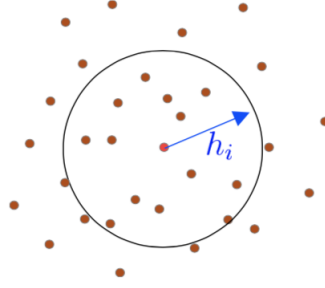


Figure 3.2: Visualization of SPH

where the integration is over the entire space, and W is an interpolating kernel with

$$\int W(\|\mathbf{r} - \mathbf{r}'\|, h) d\mathbf{r}' = 1 \quad (3.2)$$

and

$$\lim_{h \rightarrow 0} W(\|\mathbf{r} - \mathbf{r}'\|, h) d\mathbf{r}' = \delta(\|\mathbf{r} - \mathbf{r}'\|) \quad (3.3)$$

Normally, we want the kernel to be Non-negative and rotational invariant.

$$W(\|\mathbf{x}_i - \mathbf{x}_j\|, h) = W(\|\mathbf{x}_j - \mathbf{x}_i\|, h) \quad (3.4)$$

$$W(\|\mathbf{r} - \mathbf{r}'\|, h) \geq 0 \quad (3.5)$$

For numerical work, we can use midpoint rule,

$$A_I(\mathbf{x}) \approx A_S(\mathbf{x}) = \sum_i A(\mathbf{x}_i) W(\|\mathbf{x}_i - \mathbf{x}\|, h) \Delta V_i \quad (3.6)$$

Since $V_i = m_i / \rho_i$

$$A_S(\mathbf{x}) = \sum_i \frac{m_i}{\rho_i} A(\mathbf{x}_i) W(\|\mathbf{x}_i - \mathbf{x}\|, h) \quad (3.7)$$

The default, gradient and Laplacian of A are:

$$\begin{aligned} \nabla A_S(\mathbf{x}) &= \sum_i \frac{m_i}{\rho_i} A(\mathbf{x}_i) \nabla W(\|\mathbf{x}_i - \mathbf{x}\|, h) \\ \nabla^2 A_S(\mathbf{x}) &= \sum_i \frac{m_i}{\rho_i} A(\mathbf{x}_i) \nabla^2 W(\|\mathbf{x}_i - \mathbf{x}\|, h) \end{aligned} \quad (3.8)$$

3.2.2 Kernels

Smoothing kernels functions are one of the most important points in SPH. Stability, accuracy and speed of the whole method depends on these functions. Different kernels are being used for different purposes. One possibility for W is a Gaussian. However, most current SPH implementations are based on kernels with finite support. We mainly introduce gaussian, poly6 and spicky kernel here. And compare the different kernels and their property.

Poly6

The kernel is also known as the 6th degree polynomial kernel.

$$W_{poly6}(\mathbf{r}, h) = \frac{315}{64\pi h^9} \begin{cases} (h^2 - \|\mathbf{r}\|^2)^3 & 0 \leq \|\mathbf{r}\| \leq h \\ 0 & \text{Otherwise} \end{cases} \quad (3.9)$$

Then, the gradient of this kernel function can be

$$\nabla W_{poly6}(\mathbf{r}, h) = -\frac{945}{32\pi h^9} \begin{cases} \mathbf{r}(h^2 - \|\mathbf{r}\|^2)^2 & 0 \leq \|\mathbf{r}\| \leq h \\ 0 & \text{Otherwise} \end{cases} \quad (3.10)$$

The laplacian of this kernel can be expressed by,

$$\nabla^2 W_{poly6}(\mathbf{r}, h) = -\frac{945}{16\pi h^9} \begin{cases} (h^2 - \|\mathbf{r}\|^2)(3h^2 - 7\|\mathbf{r}\|^2) & 0 \leq \|\mathbf{r}\| \leq h \\ 0 & \text{Otherwise} \end{cases} \quad (3.11)$$

As Müller stated[3], if the kernel is used for the computation of pressure forces, particles tend to build cluster under high pressure because ‘as particles get very close to each other, the repulsive force vanishes because the gradient of the kernel approaches zero to the center.’, which we can see in Figure 3.4. Another kernel, spiky kernel, is proposed by Desbrum and Gascuel[4] to solve this problem.

Spicky

The kernel proposed by Desbrum and Gascuel[4]

$$W_{spiky}(\mathbf{r}, h) = \frac{15}{\pi h^6} \begin{cases} (h - \|\mathbf{r}\|)^3 & 0 \leq \|\mathbf{r}\| \leq h \\ 0 & \text{Otherwise} \end{cases} \quad (3.12)$$

Then, the gradient of spiky kernel can be described by,

$$\nabla W_{spiky}(\mathbf{r}, h) = -\frac{45\mathbf{r}}{\pi h^6 \|\mathbf{r}\|} \begin{cases} (h - \|\mathbf{r}\|)^2 & 0 \leq \|\mathbf{r}\| \leq h \\ 0 & \text{Otherwise} \end{cases} \quad (3.13)$$

The laplacian of spiky can be expressed by,

$$\nabla^2 W_{spiky}(\mathbf{r}, h) = \frac{90}{\pi h^6} \begin{cases} h - \|\mathbf{r}\| & 0 \leq \|\mathbf{r}\| \leq h \\ 0 & \text{Otherwise} \end{cases} \quad (3.14)$$

3.2.3 Grid size and smoothing length

The grid should be also fine enough to capture the variation in our simulation. In our case, it is reasonable to have a grid fine enough such that no two contact points are mapped into the same cell.

Smoothing length, h , is one of the most important parameters that affects the whole SPH method by changing the kernel value results and neighbor searching results. Too small or too big values might cause lose essential information in the simulation.

3.2.4 Neighbor Search

Neighbor search is one of the most crucial procedures in SPH method considering all interpolation equations, $A(\mathbf{r})$, needs the neighbor list for every particle (refer to equation 3.8). A naive neighbor searching approach would end up with a complexity of $O(n^2)$. The complexity

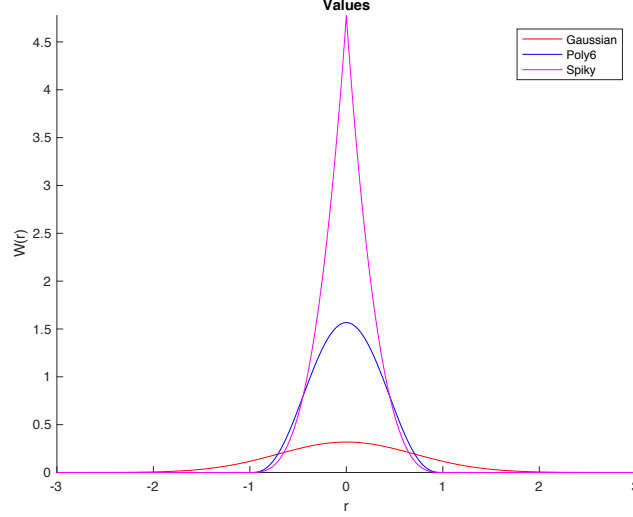


Figure 3.3: Comparison of different kernels, we set smoothing length $h = 1$ here.

is not good enough since it is impossible to reach any interactive speed when the particle count increases. With an efficient nearest neighbor searching (NNS) algorithm, it is possible to have a significant performance increase since it is the most time consuming procedure in SPH computation. In order to decrease the complexity, we choose to use $k - d$ tree data structure to store the particle spatial information and then do the nearest neighbor searching.

Hierarchical Tree

Using an adaptive hierarchy tree search is proposed by Paiva[5] to find particle neighbors. Since the simulation takes place in two dimensions, $k - d$ tree data structure was used in this approach.

An octree structure has been adapted from Macey (b) Octree Demo. The hierarchy tree is formed with a pre-defined height. The simulation box is divided recursively into eight pieces, nodes. The nodes at height = 1 are called leaves. Each node has a surrounding box for particle query which is used to check if the particle is inside the node. Each parent node, contains the elements that are divided

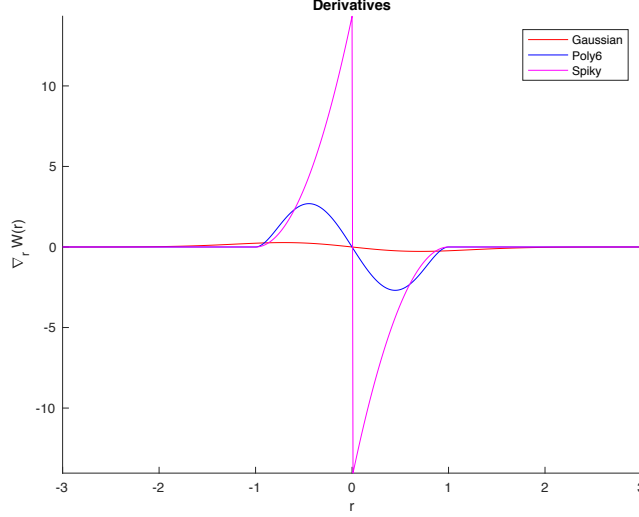


Figure 3.4: Comparison of gradient of different kernels, we set $h = 1$ here.

through its children. The particle is being checked at each level of the tree if it's intersecting the node. If it does, descend one level down in that node. After reaching to leaves, bottom level, particle has been checked if its within the search distance, h . If the particle is in the range, add it to the neighbor list. Neighbor searching is done when the whole tree has been traversed. The search distance set to be smoothing length in this implementation.

The complexity of this tree search method is $O(n \log(n))$, n being the number of particles. The performance of this algorithm is worse than Spatial Hashing method. In addition, the results obtained using this NNS algorithm wasn't accurate and stable for this implementation. Therefore as mentioned above, Spatial Hashing method was preferred.

3.3 Grid to particle

After getting the grid image for simulation state in time t , we will use the grid cells as input and renew the grid image based on trained

model. Once the grid image in $t + \Delta t$ have been renewed, the next step is to transfer the grid to particles which will instore all information including velocity,

3.3.1 Bilinear interpolation

We applied bilinear interpolation in our case, since we did mainly research on a rectilinear $2 - D$ grid. The key idea is to perform lin-

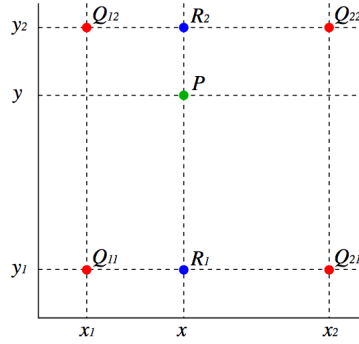


Figure 3.5: The figure shows visualiation of bilinear interpolation. The four red dots show the data points and the green dot is the point at which we want to interpolate.

ear interpolation first in one direction, and then again in the other direction. Although each step is linear in the sampled values and in the position, the interpolation as a whole is not linear but rather quadratic in the sample location.

As shown in Figure 3.5, We have known $Q_{a,b} = (x_a, y_b)$ and $a \in \{1, 2\}$ $b \in \{1, 2\}$. Then, we can firstly do linear interpolation in the x -direction. This yields

$$\begin{aligned} f(x, y_1) &\approx \frac{x_2 - x}{x_2 - x_1} f(Q_{11}) + \frac{x - x_1}{x_2 - x_1} f(Q_{21}), \\ f(x, y_2) &\approx \frac{x_2 - x}{x_2 - x_1} f(Q_{12}) + \frac{x - x_1}{x_2 - x_1} f(Q_{22}). \end{aligned} \quad (3.15)$$

After getting the two values in x -direction $f(x, y_1)$ and $f(x, y_2)$, we can use these values to do interpolation in y - direction.

$$f(x, y) \approx \frac{y_2 - y}{y_2 - y_1} f(x, y_1) + \frac{y - y_1}{y_2 - y_1} f(x, y_2) \quad (3.16)$$

Combine $f(x, y_1)$ and $f(x, y_2)$ defined in equation 3.15, we can get,

$$\begin{aligned}
f(x, y) &\approx \frac{y_2 - y}{y_2 - y_1} \left(\frac{x_2 - x}{x_2 - x_1} f(Q_{11}) + \frac{x - x_1}{x_2 - x_1} f(Q_{21}) \right) \\
&\quad + \frac{y - y_1}{y_2 - y_1} \left(\frac{x_2 - x}{x_2 - x_1} f(Q_{12}) + \frac{x - x_1}{x_2 - x_1} f(Q_{22}) \right) \\
&= \frac{1}{(x_2 - x_1)(y_2 - y_1)} \left(\begin{aligned} &f(Q_{11})(x_2 - x)(y_2 - y) + f(Q_{21})(x - x_1)(y_2 - y) \\ &+ f(Q_{12})(x_2 - x)(y - y_1) + f(Q_{22})(x - x_1)(y - y_1) \end{aligned} \right) \\
&= \frac{1}{(x_2 - x_1)(y_2 - y_1)} \begin{bmatrix} x_2 - x & x - x_1 \end{bmatrix} \\
&\quad \cdot \begin{bmatrix} f(Q_{11}) & f(Q_{12}) \\ f(Q_{21}) & f(Q_{22}) \end{bmatrix} \begin{bmatrix} y_2 - y \\ y - y_1 \end{bmatrix}
\end{aligned} \tag{3.17}$$

3.4 Conclusion

Chapter 4

Deep Learning For Simulation

4.1 Convolutional Neural Networks

4.2 CNN Constructure

4.2.1 Convolutional layers

4.2.2 Full-connected layers

4.3 Traing configuration

4.3.1 Loss Function

4.3.2 Optimizer(SGD)

4.4 Training Results

4.5 Simulation based on Trained model

Chapter 5

Implementation

Chapter 6

Conclusion

6.1 Future work

References

- [1] J. Tompson, K. Schlachter, P. Sprechmann, and K. Perlin, “Accelerating Eulerian Fluid Simulation With Convolutional Networks”, *ArXiv e-prints*, Jul. 2016. arXiv: 1607.03597 [cs.CV].
- [2] J. J. Monaghan, “Smoothed particle hydrodynamics”, *Annual review of astronomy and astrophysics*, vol. 30, no. 1, pp. 543–574, 1992.
- [3] M. Müller, D. Charypar, and M. Gross, “Particle-based fluid simulation for interactive applications”, in *Proceedings of the 2003 ACM SIGGRAPH/Eurographics symposium on Computer animation*, Eurographics Association, 2003, pp. 154–159.
- [4] M. Desbrun and M.-P. Gascuel, “Smoothed particles: A new paradigm for animating highly deformable bodies”, in *Computer Animation and Simulation’96*, Springer, 1996, pp. 61–76.
- [5] A. Paiva, F. Petronetto, T. Lewiner, and G. Tavares, “Particle-based non-newtonian fluid animation for melting objects”, in *Computer Graphics and Image Processing, 2006. SIBGRAPI’06. 19th Brazilian Symposium on*, IEEE, 2006, pp. 78–85.